

Specific heat of the $S=1$ spin-dimer antiferromagnet $\text{Ba}_3\text{Mn}_2\text{O}_8$ in high magnetic fields

H. Tsujii,^{1,2} B. Andraka,¹ M. Uchida,³ H. Tanaka,⁴ and Y. Takano¹

¹*Department of Physics, University of Florida, P.O. Box 118440, Gainesville, Florida 32611-8440*

²*RIKEN, Wako, Saitama 351-0198, Japan*

³*Department of Physics, Tokyo Institute of Technology, Meguro-ku, Tokyo 152-8551, Japan*

⁴*Research Center for Low Temperature Physics, Tokyo Institute of Technology, Meguro-ku, Tokyo 152-8551, Japan*

(Received 7 September 2005; published 28 December 2005)

We have measured the specific heat of the coupled spin-dimer antiferromagnet $\text{Ba}_3\text{Mn}_2\text{O}_8$ to 50 mK in temperature and to 29 T in the magnetic field. The experiment extends to the midpoint of the field region ($25.9 \text{ T} \leq H \leq 32.3 \text{ T}$) of the magnetization plateau at $1/2$ of the saturation magnetization, and reveals the presence of three ordered phases in the field region between that of the magnetization plateau and the low-field spin-liquid region. The exponent of the phase boundary with the thermally disordered region is smaller than the theoretical value based on the Bose-Einstein condensation of spin triplets. At zero field and 29 T, the specific-heat data show gapped behaviors characteristic of spin liquids. The zero-field data indicate that the gapped triplet excitations form two levels whose energies differ by nearly a factor of 2. At least the lower level is well localized. The data at 29 T reveal that the low-lying excitations at the magnetization plateau are weakly delocalized.

DOI: [10.1103/PhysRevB.72.214434](https://doi.org/10.1103/PhysRevB.72.214434)

PACS number(s): 75.30.Kz, 75.40.Cx, 75.50.Ee

I. INTRODUCTION

An interacting array of spin dimers, each consisting of two antiferromagnetically coupled spins, has a natural tendency to exhibit plateaus in the magnetization curve $M(H)$. This is obvious if one considers such a system of $S=1$ spins. In this case, the ground state of an isolated dimer is a spin singlet, the lowest excited state is a spin triplet, and the highest energy state is a quintet. An increasing magnetic field will cause the ground state to change from the singlet to the $S_z = +1$ triplet, and then to the $S_z = +2$ quintet, resulting in two steps in $M(H)$. A weakly coupled array of $S=1$ spin dimers will maintain this progression of the ground state and will exhibit a magnetization plateau at $m=1/2$, where $m = M/M_{\text{sat}}$ is the magnetization expressed as a fraction of the saturation value.

For one-dimensional antiferromagnets, Oshikawa, Yamanaka, and Affleck¹ have predicted that $M(H)$ can have a plateau when the condition $nS(1-m) = \text{integer}$ is satisfied. Here n is the period of the ground state. These authors have argued that the magnetization plateaus are generalized Haldane states with nonzero magnetization, implying that the transverse spin components at each plateau form a quantum spin liquid quite like that of the usual $m=0$ Haldane state. The Oshikawa-Yamanaka-Affleck theorem has been generalized to higher dimensions by Oshikawa² and refined by other authors.³

Plateaus at fractional values of saturation magnetization have been observed in Cu^{2+} -based $S=1/2$ compounds, such as the three-dimensional (3D) spin-dimer antiferromagnet NH_4CuCl_3 ,⁴ the quasi-two-dimensional (2D) orthogonal-dimer antiferromagnet $\text{Sr}_2\text{Cu}(\text{BO}_3)_2$,⁵ and the frustrated quasi-2D spin system Cs_2CuBr_4 .⁶ NH_4CuCl_3 shows distinct plateaus at $m=1/4$ and $3/4$, $\text{Sr}_2\text{Cu}(\text{BO}_3)_2$ at $m=1/8$, $1/4$, and $1/3$, and Cs_2CuBr_4 at $m=1/3$ and $2/3$. In addition, plateaus at $m=1/2$ have been observed in Ni^{2+} -based $S=1$

Heisenberg antiferromagnets with bond alternations.^{7,8}

$\text{Ba}_3\text{Mn}_2\text{O}_8$ is a new $S=1$ spin-dimer antiferromagnet, in which the interdimer coupling is expected on a structural ground to be three dimensional. The magnetization of this compound has been measured at 0.65 K as a function of the magnetic field up to 50 T in a pulsed magnet.⁹ The data exhibit a low-field $m=0$ region and an $m=1/2$ plateau, which occurs at around 29 T. In this paper, we report a determination of the magnetic phase diagram over the entire field range below the $m=1/2$ plateau, by means of specific heat measurements performed down to 50 mK in temperature. We also examine the nature of the excitations at zero field and at the $m=1/2$ plateau.

$\text{Ba}_3\text{Mn}_2\text{O}_8$ has a trigonal structure of the space group $R\bar{3}m$ with the lattice parameters $a=5.711 \text{ \AA}$ and $c=21.444 \text{ \AA}$. The manganese ions are in the unusual Mn^{5+} state, which makes $S=1$. To date, all experiments including the present work have been performed on powder samples, since no single crystal has been successfully grown to our knowledge. The magnetization measured at 0.65 K is essentially zero below $H_{c1}=9.2 \text{ T}$, where it starts to increase linearly with the magnetic field.⁹ The $m=1/2$ plateau extends from $H_{c2}=25.9 \text{ T}$ to $H_{c3}=32.3 \text{ T}$, and the saturation magnetization is reached at $H_{\text{sat}} \approx 48 \text{ T}$. The zero-field gap Δ has been estimated from H_{c1} to be $\Delta = g\mu_B H_{c1} = 12.2 \text{ K}$. From the overall shape of the magnetization curve, the strengths of the intradimer and interdimer exchanges have been determined to be $J_0=17.4 \text{ K}$ and $J_1+2(J_2+J_3)=8.3 \text{ K}$, respectively, where J_0 , J_1 , J_2 , and J_3 are the first-, second-, third-, and fourth-nearest-neighbor interactions, respectively. The edges of the magnetization plateau are sharp in spite of the powder form of the sample, indicating an isotropy of the spin Hamiltonian. In electron spin resonance, the absorption spectrum has a single Lorentzian peak with a narrow linewidth, indicating the smallness of any anisotropic exchange interaction and the good isotropy of the g factor, which is determined to

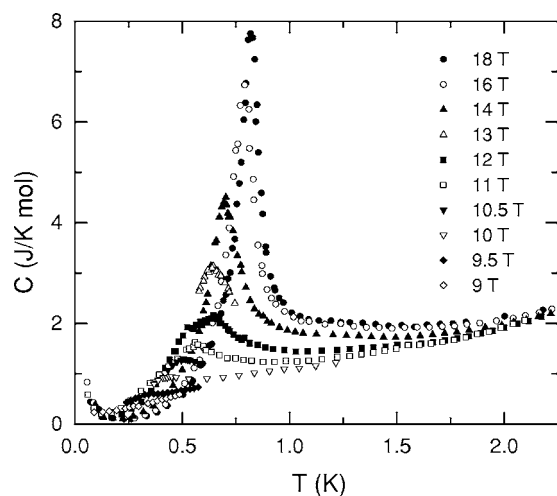


FIG. 1. Temperature dependence of the specific heat of $\text{Ba}_3\text{Mn}_2\text{O}_8$ in constant magnetic fields between 9 T and 18 T. The nuclear contribution of ^{55}Mn is visible at temperatures below 0.2 K.

be $g=1.98$.^{9,10} This g value has been used for the estimate of the gap Δ . The single-ion anisotropy term is estimated to be only $D \sim 0.02\bar{J}$ from the linewidth, where \bar{J} is the average of the exchange interactions.⁹

II. EXPERIMENTAL METHODS

The powder sample of $\text{Ba}_3\text{Mn}_2\text{O}_8$ used in the present work was synthesized by the method described in Ref. 11, with an extended sintering time of 150 h to improve the sample quality.⁹ Specific heat measurements to 18 T were performed in a superconducting magnet at temperatures down to 50 mK using a dilution refrigerator. The relaxation calorimeter for this setup has been described in Ref. 12. For measurements from 19.5 T to 29 T, another relaxation calorimeter with a built-in ^3He refrigerator was used in a resistive Bitter magnet.

Powder samples present a challenge to relaxation calorimetry at temperatures typically below 1 K because of the difficulty in obtaining a good thermal contact between the powder grains and the calorimeter. To solve this problem, we mixed the sample with a small amount of silver paint¹³ and sandwiched it between two 0.13 mm thick pieces of sapphire to form a thin, uniform layer. The bottom piece of sapphire was attached with the Wakefield compound¹⁴ to the calorimeter platform. Three samples weighing 0.15 mg, 1.08 mg, and 7.62 mg were used to cover different temperature and field regions.

III. EXPERIMENTAL RESULTS AND DISCUSSIONS

A. Magnetic phase diagram

The temperature dependence of the specific heat is shown in Fig. 1 for fields between 9 T and 18 T. In fields higher than 13 T, a well-defined peak appears in the specific heat below 1 K, signaling a phase transition. The sharpness of the peak indicates a high quality of the sample despite its powder form. An additional peak which indicates a second tran-

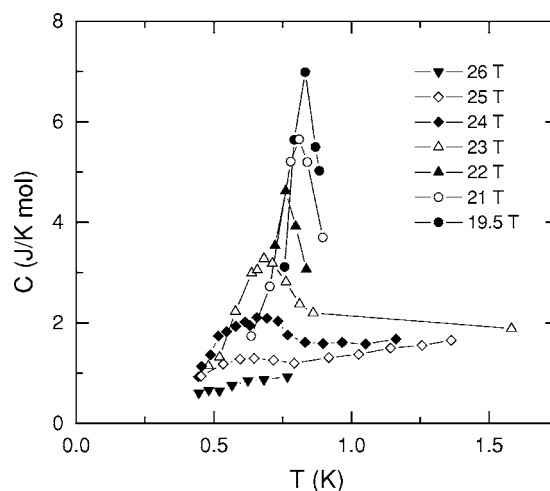


FIG. 2. Specific heat of $\text{Ba}_3\text{Mn}_2\text{O}_8$ in constant magnetic fields ranging from 19.5 T to 26 T. The lines are guides to the eye.

sition appears at 12 T. In fields lower than this value, the specific heat anomaly becomes weak, and we can identify only one peak with confidence. No peak is found at 9 T.

The specific heat in magnetic fields higher than 18 T, measured in the resistive Bitter magnet, is shown in Fig. 2. The peak in the specific heat is sharp up to 22 T. The 24 T data are very similar to the 12 T data, except that there are two shoulders instead of two peaks. At 25 T, the anomaly becomes small, and only one broad peak can be identified.

To further explore the field region below 13 T, we have measured the specific heat as a function of the magnetic field. In these measurements, a constant electric current was applied to the heater of the thermal reservoir, allowing the temperature to rise monotonically with increasing field as dictated by the magnetoresistance of the heater. As seen in Fig. 3, the phase transitions are observed as a peak and shoulder.

The magnetic phase diagram determined from the positions of the specific-heat peaks and shoulders in Figs. 1–3 is

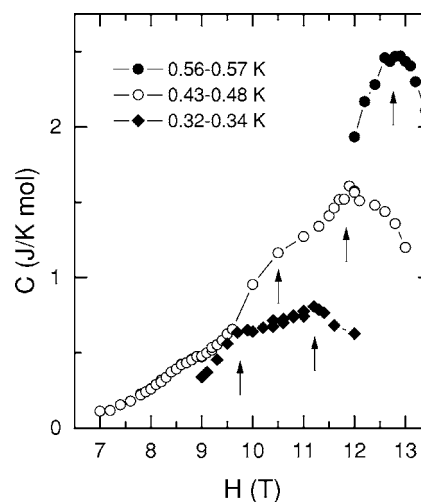


FIG. 3. Magnetic-field dependence of the specific heat of $\text{Ba}_3\text{Mn}_2\text{O}_8$. The transition points are indicated by arrows. The lines are guides to the eye.

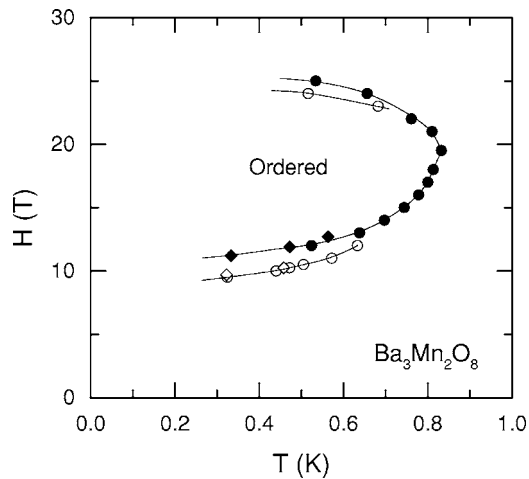


FIG. 4. Magnetic phase diagram of $\text{Ba}_3\text{Mn}_2\text{O}_8$. The circles are the positions of the peaks and shoulders in the specific heat at constant magnetic fields. The diamonds are the positions of the peaks and shoulders in the specific heat measured as a function of the magnetic field, while the current for the reservoir heater was held constant. The lines are guides to the eye.

given in Fig. 4. As seen in the figure, the transition temperatures obtained in the magnetic-field scans shown in Fig. 3 agree with those obtained in the temperature scans shown in Fig. 1. The phase diagram contains three ordered phases in the investigated field region. In addition to the H_{c1} and H_{c2} observed in the magnetization data,⁹ there are two critical fields at the intermediate fields of about 11 T and 24.5 T. Figure 4 is somewhat reminiscent of the magnetic phase diagram of CsFeBr_3 ,¹⁵ which is an $S=1$ antiferromagnet on a triangular lattice with a singlet ground state. In this material, H_c of the field-induced ordering at zero temperature splits into two branches as the temperature is raised, with the separation between the two branches widening with increasing temperature.¹⁶ In contrast, Fig. 4 suggests two branches of either H_{c1} or H_{c2} that are separate at zero temperature merging into one as the temperature is raised.

The Bose-Einstein condensation of triplets is believed to be a valid description of field-induced long-range ordering in all gapped antiferromagnets.^{17,18} According to the Bose-Einstein condensation theory, the phase boundary in the temperature vs field plot obeys a power law $T_c \propto (H - H_c)^\alpha$. The field-induced ordering in the $S=1/2$ spin-dimer material TlCuCl_3 has been interpreted in terms of the Bose-Einstein condensation.¹⁸ However, the exponent α of 0.50 determined for this material is smaller than the theoretical value of $2/3$ obtained with a Hartree-Fock approximation.

We have obtained $H_{c1} = 9.04 \pm 0.15$ T and $\alpha = 0.39 \pm 0.06$ by fitting the data of the phase boundary between the disordered phase and the ordered phase below 0.58 K. The zero-temperature critical field H_{c1} is in good agreement with 9.2 T obtained by the magnetization curve at 0.65 K. Note that the critical fields determined by a low-temperature magnetization curve $M(H)$ are generally closer to the zero-field values than the actual transition fields at the temperature of the measurement. The value for the exponent α is smaller than $2/3$ predicted by the theory. However, it agrees within the experi-

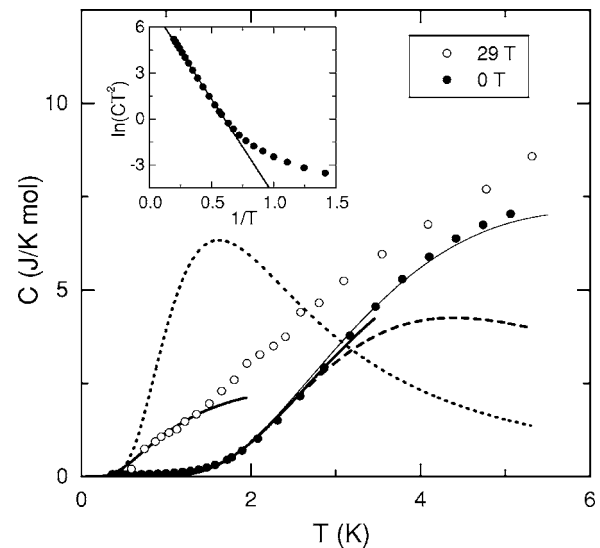


FIG. 5. Temperature dependence of the specific heat of $\text{Ba}_3\text{Mn}_2\text{O}_8$ at 0 T and 29 T. The thick solid lines are the low-temperature fits to the data. The dashed line indicates the calculated zero-field specific heat due to localized, gapped excitations, whose parameters are taken from the low-temperature fit. The thin solid line is the specific heat due to two kinds of localized excitations with two gap energies, as described in the text. The dotted line for the 29 T data indicates the specific heat of mutually isolated dimers with an excitation gap of $\Delta = 4.3$ K. In the inset, $\ln(CT^2)$ of the zero-field data have been plotted against $1/T$ to reveal the localized-excitation behavior, which is given by the straight line. The deviation of the data from the line at temperatures below 1.4 K is due to the phonon contribution and an uncertainty in the subtraction of the background heat capacity of the silver paint.

mental uncertainty with the quantum Monte Carlo result $\alpha = 0.37 \pm 0.03$ for $S=1/2$ spin dimers with a weak three-dimensional interdimer coupling.¹⁹ It is also close to the values for the $S=1$ spin-chain materials NTENP and NDMAP for the field applied parallel to the chain direction, $\alpha = 0.334 \pm 0.004$ and 0.34 ± 0.02 for NTENP (Ref. 20) and NDMAP (Ref. 21), respectively. Recently, careful analyses near the zero-temperature critical field H_{c1} have shown that the exponent α approaches $2/3$, as the temperature region of the fits is narrowed, for both the quantum Monte Carlo data²² and the experimental data²³ for TlCuCl_3 . A similar analysis has yielded $\alpha = 0.63 \pm 0.03$ for $\text{BaCuSi}_2\text{O}_6$, an $S=1/2$ spin-dimer compound with predominantly two-dimensional interdimer exchanges.²⁴ It remains to be seen, however, whether the Bose-Einstein condensation theory can explain the field-induced magnetic ordering in all gapped antiferromagnets.

B. Gapped excitations at zero field and at the magnetization plateau

In the low-field $m=0$ region, as well as at the $m=1/2$ magnetization plateau, the specific heat is expected to exhibit a gapped behavior. The data at zero field and 29 T, the mid-point of the plateau, are shown in Fig. 5. At zero field, the low-temperature behavior of the data indicates the presence

of a gap. However, the low-temperature specific heats of delocalized gapped excitations have wrong temperature dependences—see Eq. (4) for an example—which do not agree with the data. The best fit of the data below 3.5 K is obtained by using the low-temperature formula for localized gapped excitations,

$$C = \tilde{n}R(\Delta/T)^2 e^{-\Delta/T}, \quad (1)$$

where \tilde{n} is the number of excited states per spin dimer, and R is the gas constant. As shown in the inset of Fig. 5, this formula gives the best fit with an energy gap of $\Delta = 12.5 \pm 0.2$ K, which is in excellent agreement with 12.2 K estimated from H_{c1} . In $\text{Ba}_3\text{Mn}_2\text{O}_8$, the average interdimer exchange $J_1 + 2(J_2 + J_3) = 8.3$ K is substantial in comparison with the intradimer exchange $J_0 = 17.4$ K, as we have described. It is surprising that, despite such strong interdimer exchanges, the triplet excitations remain localized instead of becoming highly dispersive. The crystal structure⁹ of $\text{Ba}_3\text{Mn}_2\text{O}_8$ suggests that the localization arises from a geometric frustration.

Another surprising result of the low-temperature fit is that \tilde{n} is only 1.44 ± 0.04 , which is very close to $1/2$ of $\tilde{n} = 3$ expected for the triplets. The dashed line in the main panel of the figure shows the contribution of local excitations for the entire temperature range of the data, according to the complete expression

$$C = \tilde{n}R \frac{(\Delta/T)^2 e^{-\Delta/T}}{(1 + \tilde{n}e^{-\Delta/T})^2}, \quad (2)$$

for $\tilde{n} = 1.44$ and $\Delta = 12.5$ K found by the low-temperature fit. Above 3.5 K, the specific heat is substantially larger than can be accounted for by these excitations, strongly suggesting that the excess arises from the “missing” triplets whose gap is considerably larger than 12.5 K. Indeed, as shown by the thin solid line, the data over the entire temperature range can be well described by $1/2$ of the triplets at $\Delta = 12.5 \pm 0.2$ K and the other $1/2$ at $\Delta' = 24.5 \pm 0.5$ K,

$$C = \tilde{n}R \frac{(\Delta/T)^2 e^{-\Delta/T} + (\Delta'/T)^2 e^{-\Delta'/T} + \tilde{n}(\Delta'/T - \Delta/T)^2 e^{-(\Delta+\Delta')/T}}{[1 + \tilde{n}(e^{-\Delta/T} + e^{-\Delta'/T})]^2}, \quad (3)$$

where $\tilde{n} = 1.5$. We find $\Delta' = 2\Delta$ within the combined uncertainties of the fitting parameters. Although Eq. (3) assumes that the excitations at Δ' are localized like those at Δ , the data do not tell whether this is the case, since the excitations at Δ dominates the low-temperature behavior which distinguishes localized excitations from dispersive excitations.

The field of 29 T is located at the midpoint of the $m = 1/2$ magnetization plateau within the uncertainty of the magnetization data. As expected, no sign of ordering is observed in the specific-heat data at this field, indicating that the plateau region is a spin-liquid phase, although there is a substantial scatter at high temperatures. At the midpoint of an $m = 1/2$ magnetization plateau, mutually isolated $S = 1$

dimers will have the lowest excited level containing two states, a singlet and an $S_z = 2$ quintet. The gap for the level of the collective excitations analogous to such single-dimer states can be estimated from the width of the magnetization plateau to be $\Delta = g\mu_B(H_{c3} - H_{c2})/2 = 4.3$ K. The specific heat due to localized gapped excitations with $\tilde{n} = 2$ and $\Delta = 4.3$ K, shown by the dotted line, completely fails to describe the data at 29 T. The comparison of the line with the data in fact indicates that the energy of the excitations has a wide distribution, suggesting that their dispersion cannot be neglected in comparison with the gap size.

By following the method described by Troyer *et al.*²⁵ for one-dimensional excitations, one can derive the low-temperature expression

$$C = n_m R \frac{\Delta^2}{(4\pi a)^{3/2} T^{1/2}} e^{-\Delta/T}, \quad (4)$$

for the specific heat due to three-dimensional excitations whose gapped dispersion is $\epsilon = \Delta + a(k - k_0)^2$. Here n_m is the number of the gapped modes. This expression gives the best fit to the data below 1.5 K as shown in Fig. 5, with $\Delta = 1.9 \pm 0.1$ K, which is considerably smaller than 4.3 K anticipated by the simple argument given above. The strength of the dispersion can be estimated from the fitting parameter $a/n_m^{2/3} = 0.20 \pm 0.01$ K. Regardless of the number of modes n_m , which we do not know at the moment, this is a rather small value, indicating that the low-lying excitations at the $m = 1/2$ magnetization plateau are nearly localized, similar to the low-lying excitations at zero field. The measured specific heat continues to rise above 1.5 K, where the low-temperature approximation is invalid, revealing the presence of at least another low-lying mode whose energy is on the order of 10 K. This observation, together with the experimentally obtained value for Δ being considerably smaller than the value estimated from the plateau width, suggests that the levels of the singlet and the $S_z = 2$ quintet do not cross each other at the midpoint of the magnetization plateau.

IV. CONCLUSIONS

In this work, we have determined the magnetic phase diagram of $\text{Ba}_3\text{Mn}_2\text{O}_8$ by using specific-heat measurements to 50 mK in temperature and to 29 T in the magnetic field. The phase diagram reveals the existence of three ordered phases between the low-field spin-liquid region and the $m = 1/2$ magnetization plateau. We have found that the exponent for the transition temperature of the field-induced ordering in the investigated temperature region is clearly less than $2/3$ expected by the Bose-Einstein condensation theory.

In the spin-liquid phase at zero field, the specific heat over the entire temperature range is well accounted for by two excitation levels, each probably containing the same number of states. The gap Δ for the lower level agrees well with the value estimated from H_{c1} , and the excitations at this level are well localized. The existence of the higher level at about 2Δ

requires direct confirmation by ESR or inelastic neutron scattering.

In the spin-liquid phase at the $m=1/2$ magnetization plateau, the low-lying excitations are delocalized, but the dispersion is weak. Contrary to a naive expectation, the two collective modes arising from the singlet and the $S_z=2$ quintet of a single dimer do not cross each other at the midpoint of the plateau. We hope this finding will stimulate further theoretical work on three-dimensionally coupled spin dimers. In addition, it will be useful to perform an ESR experiment to map the excitation energies in the magnetization plateau region as a function of field.

ACKNOWLEDGMENTS

The authors thank M. Takigawa for useful information on the hyperfine field of ^{55}Mn , and F. C. McDonald, Jr., T. P. Murphy, E. C. Palm, and C. R. Rotundu for assistance. This work was supported by the NSF through Grant No. DMR-9802050 and the DOE under Grant No. DE-FG02-99ER45748. A portion of it was performed at the National High Magnetic Field Laboratory, which is supported by NSF Cooperative Agreement No. DMR-0084173 and by the State of Florida.

-
- ¹M. Oshikawa, M. Yamanaka, and I. Affleck, Phys. Rev. Lett. **78**, 1984 (1997).
²M. Oshikawa, Phys. Rev. Lett. **84**, 1535 (2000).
³G. Misguich, C. Lhuillier, M. Mambrini, and P. Sindzingre, Eur. Phys. J. B **26**, 167 (2002).
⁴W. Shiramura, K. Takatsu, B. Kurniawan, H. Tanaka, H. Uekusa, Y. Ohashi, K. Takizawa, H. Mitamura, and T. Goto, J. Phys. Soc. Jpn. **67**, 1548 (1998).
⁵H. Kageyama, K. Yoshimura, R. Stern, N. V. Mushnikov, K. Onizuka, M. Kato, K. Kosuge, C. P. Slichter, T. Goto, and Y. Ueda, Phys. Rev. Lett. **82**, 3168 (1999).
⁶T. Ono, H. Tanaka, O. Kolomiyets, H. Mitamura, T. Goto, K. Nakajima, A. Oosawa, Y. Koike, K. Kakurai, J. Klenke, P. Smeibidle, and M. Meissner, J. Phys.: Condens. Matter **16**, S773 (2004).
⁷Y. Narumi, M. Hagiwara, R. Sato, K. Kindo, H. Nakano, and M. Takahashi, Physica B **246-247**, 509 (1998).
⁸Y. Narumi, K. Kindo, M. Hagiwara, H. Nakano, A. Kawaguchi, K. Okunishi, and M. Kohno, Phys. Rev. B **69**, 174405 (2004).
⁹M. Uchida, H. Tanaka, H. Mitamura, F. Ishikawa, and T. Goto, Phys. Rev. B **66**, 054429 (2002).
¹⁰M. Uchida, H. Tanaka, M. I. Bartashevich, and T. Goto, J. Phys. Soc. Jpn. **70**, 1790 (2001).
¹¹M. T. Weller and S. J. Skinner, Acta Crystallogr., Sect. C: Cryst. Struct. Commun. **55**, 154 (1999).
¹²H. Tsujii, B. Andraka, E. C. Palm, T. P. Murphy, and Y. Takano, Physica B **329-333**, 1638 (2003).
¹³Arzerite VL-10, Tamura Kaken Corp., Sayamagahara 16-2, Iruma, Saitama, 358-8501 Japan.
¹⁴Wakefield 120 silicon compound, Wakefield Thermal Solution, Pelham, New Hampshire 03076.
¹⁵Y. Tanaka, H. Tanaka, T. Ono, A. Oosawa, K. Morishita, K. Iio, T. Kato, H. A. Katori, M. I. Bartashevich, and T. Goyo, J. Phys. Soc. Jpn. **70**, 3068 (2001).
¹⁶T. Nakamura, T. Ishida, Y. Fujii, H. Kikuchi, M. Chiba, T. Kubo, Y. Yamamoto, and H. Hori, Physica B **329-333**, 864 (2003).
¹⁷T. Giamarchi and A. M. Tsvelik, Phys. Rev. B **59**, 11398 (1999).
¹⁸T. Nikuni, M. Oshikawa, A. Oosawa, and H. Tanaka, Phys. Rev. Lett. **84**, 5868 (2000).
¹⁹S. Wessel, M. Olshanii, and S. Haas, Phys. Rev. Lett. **87**, 206407 (2001).
²⁰N. Tateiwa, M. Hagiwara, H. Aruga Katori, and T. C. Kobayashi, Physica B **329-333**, 1209 (2003).
²¹H. Tsujii, Z. Honda, B. Andraka, K. Katsumata, and Y. Takano, Phys. Rev. B **71**, 014426 (2005).
²²O. Nohadani, S. Wessel, B. Normand, and S. Haas, Phys. Rev. B **69**, 220402(R) (2004).
²³Y. Shindo and H. Tanaka, J. Phys. Soc. Jpn. **73**, 2642 (2004).
²⁴S. E. Sebastian, P. A. Sharma, M. Jaime, N. Harrison, V. Correa, L. Balicas, N. Kawashima, C. D. Batista, and I. R. Fisher, Phys. Rev. B **72**, 100404(R) (2005).
²⁵M. Troyer, H. Tsunetsugu, and D. Würtz, Phys. Rev. B **50**, 13515 (1994).